Folding model optical potentials for ^{90}Zr, ^{144}Sm and ^{208}Pb

H. L. Clark, Y.-W. Lui and D.H. Youngblood

In this report, we apply the folding model to the giant resonance data for ^{90}Zr, ^{144}Sm and ^{208}Pb reported in Ref. [1]. Optical potentials used in the analysis were determined by fitting newly measured elastic scattering data. The data extended over the range of $1.5° \leq \theta_{lab} \leq 36°$ and displayed the beginning of rainbow scattering. The differential cross sections for the low-lying 2^+ and/or 3^- states were also extracted from the data. The folding model optical potentials were tested by calculating the cross sections for these states and comparing the deduced transition rates with accepted values.

Beams of 240 MeV alpha particles from the Texas A&M K500 superconducting cyclotron bombarded self-supporting ^{90}Zr, ^{144}Sm and ^{208}Pb foils mounted in the target chamber of the multipole-dipole-multipole spectrometer. The thickness of the targets were 3.80, 6.90 and 11.84 mg/cm^2, respectively, and all were enriched to >95%. The focal plane detector consisted of four 60 cm long proportional counters (separated by 13.55 cm) to measure x-position and θ, an ionization chamber to measure ΔE, and a scintillator to measure E and to provide a fast trigger. The angle θ was calibrated by using a collimator with five 0.1° slit openings at -2, -1, 0, 1, and 2°. The principals of operation are similar to the detector in Ref. [2].

The ^{208}Pb data were taken at spectrometer angles of 3.5, 5, 7, 9, 11, 13, 16, 19, 22, 26, 29, and 32° with a spectrometer acceptance of $\Delta\theta = \pm 2.0°$ and $\Delta\phi = \pm 0.8°$. The ^{90}Zr and ^{144}Sm data were taken during a later run at spectrometer angles of 4, 6, 8, 10, 12, 15, 18, 21, 25, 28 and 31° with a spectrometer acceptance of $\Delta\theta = \pm 2.0°$ and $\Delta\phi = \pm 0.8°$ and at 33° and 36° with a larger acceptance of $\Delta\theta = \pm 2.0°$ and $\Delta\phi = \pm 2.0°$. In the analysis, software cuts on θ were applied to divide each data set into ten angle bins, each corresponding to $\Delta\theta \approx 0.4°$. The average angle for each bin was determined by averaging over the height of the solid angle defining slit and the width of the angle bin. For each angle bin, the elastic and inelastic scattering peak positions, widths, and cross

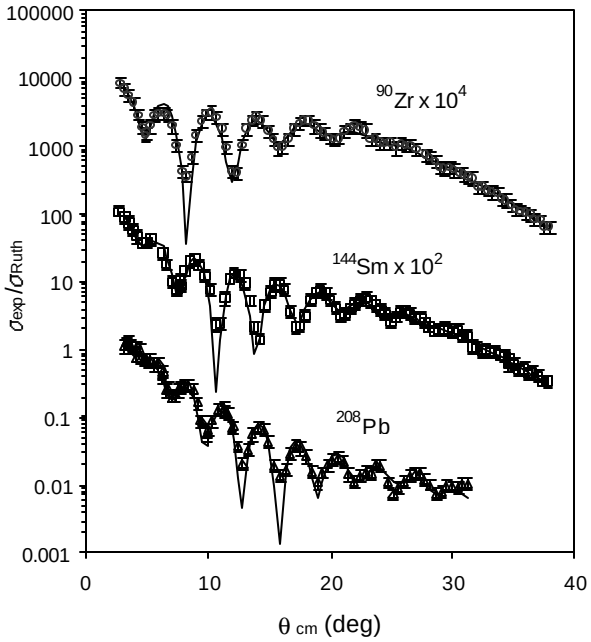

Figure 1. Angular distribution of the ratio of elastic scattering differential cross section to Rutherford scattering for 240 MeV α particles on ^{90}Zr, ^{144}Sm and ^{208}Pb plotted versus average center-of-mass angle. The folding model parameters used are given in Table I.

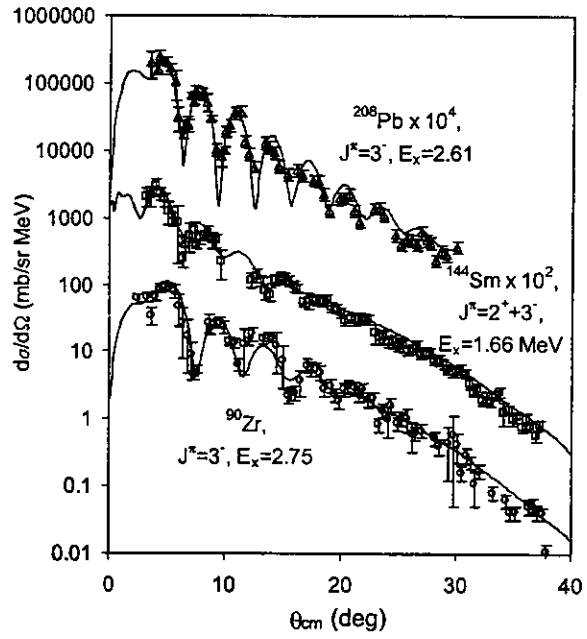

Figure 2. Inelastic scattering differential cross sections obtained for states indicated for ^{90}Zr, ^{144}Sm and ^{208}Pb excited by 240 MeV α particles plotted versus average center-of-mass angle. The calculations were made using the folding model parameters from Table I and accepted transition rates from Table II.

mass angle in Figs. 1 and 2. The error bars represent the combined uncertainty from statistical, systematic and angle error summed in quadrature. Absolute cross sections were obtained from the combination of charge integration, target thickness, solid angle, and dead time. Data from a monitor detector, fixed at θ_{lab}=20°, were used to verify the normalizations between the different data sets across the entire angular range.

Optical model parameters were determined by fitting the data with the code PTOLEMY [3]. The folding model used to describe the interaction assumed a density-dependent, Gaussian-shaped, α-nucleon interaction to describe the real part of the potential and used a Woods-Saxon expression for the imaginary part of the potential. This form has been applied previously to describe 240 MeV alpha particle scattering of ^{58}Ni and ^{116}Sn and the details of the model and calculations with PTOLEMY are described thoroughly in Refs. [4,5]. The lines in Fig. 1 show the calculated angular distributions. Table I lists the parameters obtained from the fits to the data from this analysis and the optical model parameters used for the previous giant resonance analysis [1,5,6].

Using the folding model parameters in Table I, coupled-channel distorted-wave Born approximation calculations were carried out with PTOLEMY for the low-lying states and giant resonances. The expressions used for the sum rules and transition rates were obtained from Refs. [6,7]. The transition rates for the low-lying states were deduced from fits of the calculated angular distributions to the data. Figure 2 shows the calculated angular distributions for the low-lying states using accepted values [8] for the transition rates. Both the accepted and deduced values for the transition rates are listed in Table II. The experimental errors represent fits to the data where χ^2 changed by a factor of 2.

Folding model optical parameters were obtained for 240 MeV alpha particle scattering on ^{90}Zr, ^{144}Sm and ^{208}Pb. The potentials were verified by comparing calculated cross sections for low-lying states to data. The deduced

Table I. Folding optical model parameters (F) obtained from fits to elastic scattering data. The DP parameters are the Woods-Saxon optical model parameters used in the previous giant resonance analysis [1,5,6].

nuclei	model	v (MeV)	V (MeV)	R_v	a_v (fm)	W (MeV)	R_w	a_w (fm)
^{90}Zr	F	41.8				31.1	0.898	1.05
	DP		88.0	0.893	0.830	21.4	1.07	0.800
^{144}Sm	F	43.2				34.9	0.958	0.963
	DP		88.6	0.930	0.747	23.3	1.07	0.837
^{208}Pb	F	39.0				18.0	1.13	0.813
	DP		80.2	0.970	0.800	36.6	1.04	0.750

Table II. Accepted [8] and experimental transition rates for low-lying states. The experimental values were deduced using folding model calculations.

nuclei	Ex (MeV)	$J^\pi=2^+$, B(E2) (e^2b^2)		$J^\pi=3^-$, B(E3) (e^2b^3)	
		Accep.	Exp.	Accep.	Exp.
^{90}Zr	2.75			0.0517 ±0.0181	0.046 ±0.010
^{144}Sm	1.66	0.275 ±0.014	0.27 ±0.05	0.270 ±0.013	0.22 ±0.05
^{208}Pb	2.61			0.614 ±0.011	0.61 ±0.06

transition rates were found to agree with accepted values to within error.

Cross sections for the giant resonance data of Ref. [1] were also calculated with the folding potentials obtained. Figure 3 illustrates the cross sections obtained from folding and DP models for ^{208}Pb assuming each transition exhausted the full energy-weighted sum rule (EWSR) limit. Comparisons of the two models between $0 \le \theta_{cm} \le 6°$ show that the angular distributions of the giant monopole resonance (GMR) have, in general, the same shape and

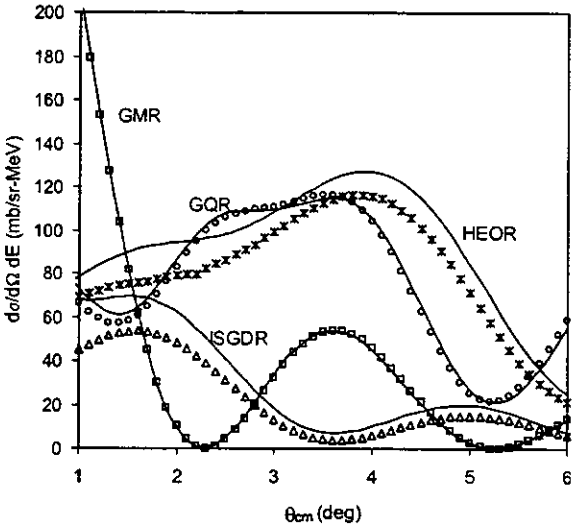

Figure 3. Inelastic scattering differential cross sections obtained for giant resonances indicated for ^{208}Pb excited by 240 MeV α particles plotted versus average center-of-mass angle. Calculations made with the DP and folding parameters from Table I are represented by the solid lines and symbols, respectively. The calculations were made assuming that each transition exhausted the full EWSR limit.

Table III. Ratio of calculated DP to folding model cross sections. The calculations were made assuming that each transition exhausted the full EWSR limit.

nuclei	GMR	ISGDR	GQR	HEOR
^{90}Zr	1.01	1.00	1.18	1.35
^{144}Sm	0.99	0.93	0.88	0.98
^{208}Pb	1.02	1.27	1.05	1.12

magnitude. The calculated cross sections for the giant quadrupole resonance (GQR), high-energy octupole resonance (HEOR) and isoscalar giant dipole resonance (ISGDR) were found to have both different shapes and magnitudes. Table III lists the ratio of the calculated DP to folding model cross sections for each nuclei. The sensitivity of the calculated giant resonance cross sections to variations of the folding model parameters is presently under investigation.

[1] H.L. Clark, Y.-W. Lui, D.H. Youngblood, Nucl. Phys. **A649**, 57c (1999).

[2] D.H. Youngblood, Y.-W. Lui, H.L. Clark, P. Oliver, and G. Simler, Nucl. Instr. Meth. Phys. Res., Sect. **A361**, 539 (1995).

[3] M. Rhoades-Brown, M.H. Macfarlane, and S.C. Pieper, Phys. Rev. C **21**, 2417 (1980); 2436; M.H. Macfarlane and S.C. Pieper, Argonne Nat. Lab. Rep. No. ANL-76-11, Rev. 1 (1978).

[4] G.R. Satchler and D.T. Khoa, Phys. Rev. C **55**, 285 (1997).

[5] H.L. Clark, D.H. Youngblood, and Y.-W. Lui, Phys. Rev. C **57**, 2887 (1998).

[6] H.L. Clark, D.H. Youngblood, and Y.-W. Lui, Nucl. Phys. **A589**, 416 (1995).

[7] G.R.Satchler, Nucl. Phys. **A472**, 215 (1987).

[8] NNDC Nuclear Data Tables, Brookhaven National Laboratory.